Available online at www.sciencedirect.com
ScienceDirect
Journal of Sound and Vibration 303 (2007) 455–474
JOURNAL OF SOUND AND VIBRATION
www.elsevier.com/locate/jsvi

A simultaneous equation method-based online secondary path modeling algorithm for active noise control

Guo-yong Jin*, Tie-jun Yang, You-hong Xiao, Zhi-gang Liu

School of Power and Energy Engineering, Harbin Engineering University, Harbin, Hei Longjiang 150001, PR China

Received 12 April 2005; received in revised form 12 May 2006; accepted 13 November 2006
Available online 28 March 2007

Abstract

Existing conventional online secondary path modeling algorithms for active noise control system have the characteristic that the operation of the controller and the modeling process of the secondary path are mutually interfered. So this unwanted interference will degrade the noise-reducing performance and even the stability of the system. A new finite impulse response (FIR) filter-based online secondary path identification algorithm is proposed to eliminate the interactive disturbances. Compared with existing algorithms, the proposed method does not need feeding extra noise to the secondary source, and is also different from the overall modeling method using the control output. Instead, the facts that the FIR filters have coefficient vectors equivalent to impulse responses corresponding to the transfer functions of physical systems are utilized, and when the coefficients of the control filter are updated, the filter coefficient vectors are different at different iteration steps because of estimation errors. Furthermore, in the method, the modeling of the secondary path is relatively independent of the active noise control system, and the reference signal is used as the input for the system identification. Therefore, the unwanted disturbances between the operation of the ANC controller and the identification of the secondary path are eliminated completely, and the complexity of ANC system is greatly reduced. Computer simulations show its effectiveness, robustness, and the advantage of low residual noise.

1. Introduction

The filtered-X LMS (FXLMS) algorithm is one of the most popular adaptive filtering algorithms in active noise control because of its simplicity, robustness and relatively low computational load. As an extension of LMS algorithm for ANC systems, the FXLMS algorithm takes account of the presence and influence of the secondary path transfer function between the output of the control filter and the error sensor. The block diagram of the ANC system with FXLMS algorithm is illustrated in Fig. 1 [1]. In this figure, $S(z)$ is the transfer function of the secondary path which comprises the D/A converter, smoothing filter, power amplifier, secondary loudspeaker, acoustic path from the loudspeaker to error microphone, error microphone, anti-aliasing filter, and A/D converter. In order to compensate the influence of the secondary path, the reference signal must be filtered by the secondary path transfer function estimation $\hat{S}(z)$, and the modeling error

*Corresponding author. Tel./fax: +86 451 82518264.
E-mail address: jgy1822@yahoo.com.cn (G.-y. Jin).

0022-460X/$ - see front matter © 2007 Elsevier Ltd. All rights reserved.
doi:10.1016/j.jsv.2006.11.039

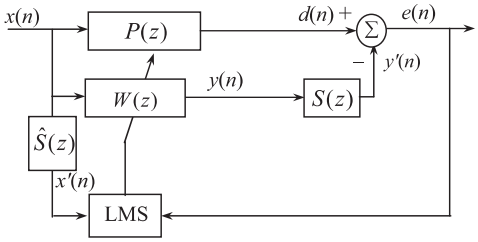

Fig. 1. Block diagram of ANC system with FXLMS algorithm.

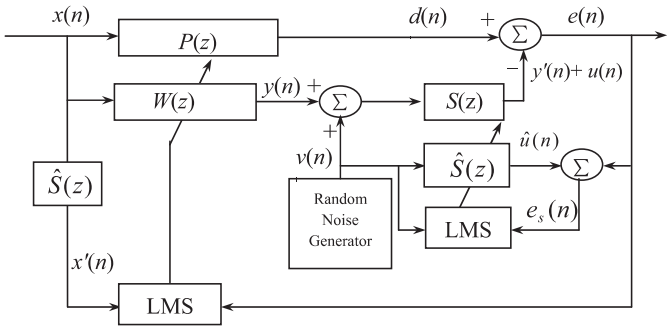

Fig. 2. Block diagram of active control system with online secondary path modeling using additive random noise (Eriksson's method).

between the secondary path and its estimated model will affect the noise attenuation performance and stability of the algorithm. Only if the phase difference between the secondary path and the estimated model is less than 90°, the stable convergence of filtered-X LMS algorithm can be guaranteed [2,3]. Therefore, it is very important for an ANC system that the model of the secondary path be estimated fast and precisely.

If the secondary path is unchanged during the operation of an ANC system, the secondary path can be modeled offline, and then the estimated secondary path coefficients can be used with the ANC system turned on. However, in some practical cases, the secondary path may be time varying. The change degrades the noise-reducing performance and even the stability of the system. So offline modeling of the secondary path cannot satisfy the robust requirement of the control system. It is necessary and practical to model secondary path online to ensure the convergence of FXLMS algorithm.

A number of algorithms for online secondary path modeling have been proposed [4–14]. These methods can be divided into two types. The first approach, as shown in Fig. 2, involving the injection of additional random white noise, which is uncorrelated with the primary noise $x(n)$ into the ANC system, utilizes a system identification method to estimate the secondary path [4]. The second one, as shown in Fig. 3, called the overall modeling algorithm, uses the output of the controller to model $S(z)$ [8].The first approach provides a signal-independent modeling, so the model obtained is valid for the entire frequency range of interest. It has been concluded [8] that the first approach is superior to the second approach on convergence rate, speed of response to changes of primary noise, updating duration, computational complexities. Therefore, the first approach has been developed greatly in the last decade. Nevertheless, mutual disturbances between the operation of ANC controller and the modeling of secondary path always exist in the first approach [7], and the prominent problem is that the injection of a random noise will increase the residual noise level, which cannot be suppressed by controller. Although the problem can be mitigated by reducing the power of the injected noise, the convergence rate and precision of the secondary path modeling are decreased. Compared with the first approach, the second approach does not need feeding extra noise to the ANC system. But this method involves signal-dependent modeling [8]. It can be seen from Fig. 3 that the reference input $x(n)$ of the filter $\hat{S}(z)$ is correlated with the input $y(n)$ of the filter $\hat{P}(z)$, so it does not always produce correct model unless some conditions are satisfied and certain precautions are taken. The second approach was analyzed theoretically in Ref. [10], and the conditions that the noise control filter should satisfy for optimal online modeling were obtained. A detailed comparison of the two online modeling approaches can be found in Ref. [8]. To reduce

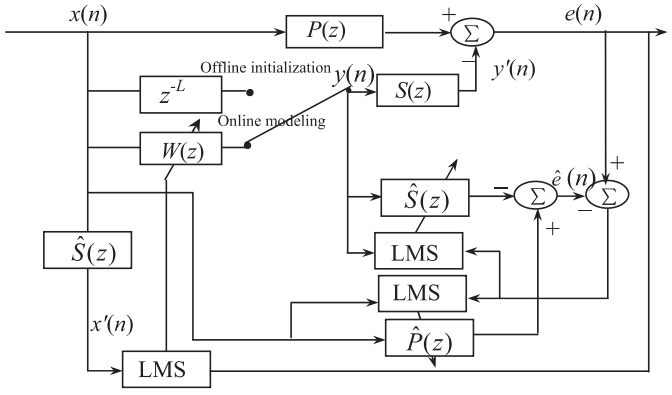

Fig. 3. Block diagram of active control system with online secondary path modeling using overall modeling strategy.

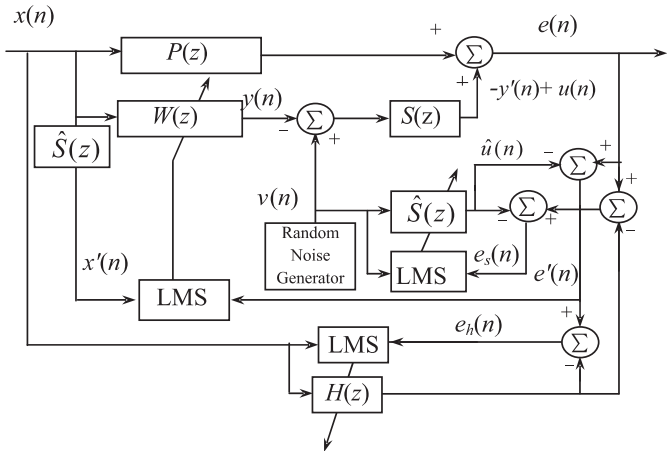

Fig. 4. Block diagram of cross-updated active control system with improved online secondary path modeling using additive random noise (Zhang's method).

the undesirable interferences between the operation of the ANC controller and the modeling of secondary path, several improved techniques have been proposed [5–7,11–13]. Two different methods [5,6] were utilized to reduce the interference of the active control process in the modeling process, respectively, while [7] focused on reducing the mutual interferences between the modeling process and the operation of the ANC controller by using three cross-updated adaptive filters, as illustrated in Fig. 4. The performance of both modeling and noise reduction has been shown to be greatly improved. On the basis of Ref. [7], a new technique is proposed in Ref. [11], aiming at decreasing the residual noise level by using the varying auxiliary noise according to the working status of the ANC system. The convergence rate and whole performance of ANC system with online secondary path modeling using the injection of a random noise were further improved in Ref. [13].

From the literature review above, it is known that two existing online modeling approaches of secondary path have been developed, the performance of ANC system with online secondary path modeling has been improved to a large extent. However, the mutual disturbances between the operation of the ANC and the identification of the secondary path cannot be eliminated radically. Therefore, the performance of the whole ANC system is limited.

In this paper, a new online secondary path modeling algorithm is proposed. It is based on the simultaneous equation method proposed by Fujii et al. [15,16]. Based on the principle of the simultaneous equation method, the proposed method utilizes the facts that the finite impulse response (FIR) filters have coefficient vectors equivalent to impulse responses corresponding to the transfer functions of physical systems, and when the

coefficients of control filter are updated, the filter coefficient vectors are different at different iteration steps to derive two independent equations which contain the primary path and secondary path online. The secondary path impulse response is derived by solving the two equations. Using the reference signal as the input for the system identification, a new system identification technique is adopted to solve the simultaneous equations, and the modeling of the secondary path is relatively independent of the active noise control system. The paper is organized as follows. In Section 2, the proposed algorithm is developed and described. In Section 3, the effect of parameter selection on the algorithm is discussed. Finally, simulation results are presented and discussed to demonstrate the effectiveness of the proposed algorithm followed by the conclusions.

2. Description of the algorithm

2.1. Principle

The block diagram of the simultaneous equation method is illustrated in Fig. 5. In this figure, the term, $H(z)$, is the transfer function of an additional filter that models the overall path from the detection sensor to the error sensor; $P(z)$ is the transfer function of the primary path; $S(z)$ is the transfer function of the secondary path. For any $W(z)$, in the ideal case that the overall path is modeled by $H(z)$ precisely, the equation is derived as

$$H(z) = P(z) - W(z)S(z). \tag{1}$$

So when two different transfer functions of the noise control filter $W(z)$, expressed as $W(1, z)$ and $W(2, z)$, are set arbitrarily, the additional filter yields two equations related to each transfer function

$$H(1, z) = P(z) - W(1, z)S(z) \tag{2}$$

and

$$H(2, z) = P(z) - W(2, z)S(z). \tag{3}$$

Obviously, eliminating $P(z)$ from Eqs. (2) and (3) yields the solution

$$S(z) = \frac{H(1, z) - H(2, z)}{W(2, z) - W(1, z)} \tag{4}$$

if $W(1, z) \neq W(2, z)$.

Practically, all filters are generally formed as FIR filters. So the transfer functions $H(z)$, $W(z)$ and $S(z)$ can be, respectively, expressed as

$$H(z) = h_0 + h_1 z^{-1} + h_2 z^{-2} + \cdots + h_{N-2} z^{-(N-2)} + h_{N-1} z^{-(N-1)}, \tag{6}$$

$$W(z) = w_0 + w_1 z^{-1} + w_2 z^{-2} + \cdots + w_{M-2} z^{-(M-2)} + w_{M-1} z^{-(M-1)} \tag{7}$$

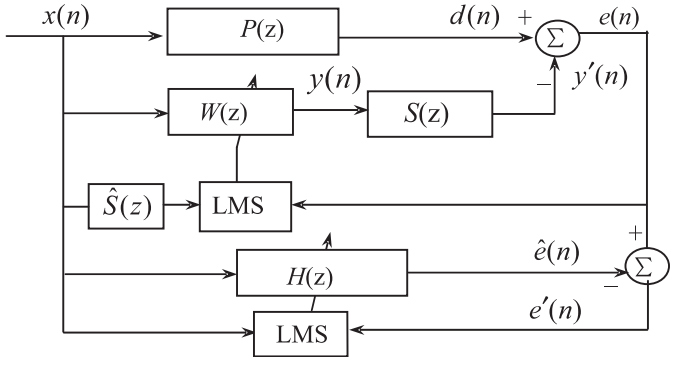

Fig. 5. Block diagram of the principle of the simultaneous equation method.

and

$$S(z) = s_0 + s_1 z^{-1} + s_2 z^{-2} + \cdots + s_{L-2} z^{-(L-2)} + s_{L-1} z^{-(L-1)}, \tag{8}$$

where N, M and L are the corresponding filter length.

Fortunately, this type of filter has coefficient vectors equivalent to impulse responses corresponding to transfer functions. The transfer functions $H(z)$, $W(z)$ and $S(z)$, are hence expressed as coefficient vectors:

$$\mathbf{H} = \begin{bmatrix} h_0 & h_1 & \cdots & h_{N-1} \end{bmatrix}^{\mathrm{T}}, \tag{9}$$

$$\mathbf{W} = \begin{bmatrix} w_0 & w_1 & \cdots & w_{M-1} \end{bmatrix}^{\mathrm{T}} \tag{10}$$

and

$$\mathbf{S} = \begin{bmatrix} s_0 & s_1 & \cdots & s_{L-1} \end{bmatrix}^{\mathrm{T}}. \tag{11}$$

Similarly, $W(1, z)$, $W(2, z)$, $H(1, z)$, and $H(2, z)$are expressed as

$$\mathbf{W}(1) = \begin{bmatrix} w_0(1) & w_1(1) & \cdots & w_{M-1}(1) \end{bmatrix}^{\mathrm{T}}, \tag{12}$$

$$\mathbf{W}(2) = \begin{bmatrix} w_0(2) & w_1(2) & \cdots & w_{M-1}(2) \end{bmatrix}^{\mathrm{T}}, \tag{13}$$

$$\mathbf{H}(1) = \begin{bmatrix} h_0(1) & h_1(1) & \cdots & h_{N-1}(1) \end{bmatrix}^{\mathrm{T}} \tag{14}$$

and

$$\mathbf{H}(2) = \begin{bmatrix} h_0(2) & h_1(2) & \cdots & h_{N-1}(2) \end{bmatrix}^{\mathrm{T}}. \tag{15}$$

According to Eqs. (12)–(15), (6) and (7), $H(1,z)-H(2,z)$ and $W(2,z)-W(1,z)$ in Eq. (4) can be transformed to the differences between coefficient vectors, respectively:

$$\begin{aligned} \mathbf{\Delta H} &= \mathbf{H}(1) - \mathbf{H}(2) \\ &= \begin{bmatrix} h_0(1) - h_0(2) & h_1(1) - h_1(2) & \cdots & h_{N-1}(1) - h_{N-1}(2) \end{bmatrix}^{\mathrm{T}} \\ &= \begin{bmatrix} \Delta h_0 & \Delta h_1 & \cdots & \Delta h_{N-1} \end{bmatrix}^{\mathrm{T}} \end{aligned} \tag{16}$$

and

$$\begin{aligned} \mathbf{\Delta W} &= \mathbf{W}(2) - \mathbf{W}(1) \\ &= \begin{bmatrix} w_0(2) - w_0(1) & w_1(2) - w_1(1) & \cdots & w_{M-1}(2) - w_{M-1}(1) \end{bmatrix}^{\mathrm{T}} \\ &= \begin{bmatrix} \Delta w_0 & \Delta w_1 & \cdots & \Delta w_{M-1} \end{bmatrix}^{\mathrm{T}}. \end{aligned} \tag{17}$$

Note that Eq. (4) can be rewritten as

$$\{W(2,z) - W(1,z)\} S(z) = H(1,z) - H(2,z). \tag{18}$$

Since the multiplication of transfer functions in Eq. (18) corresponds to the convolution of impulse responses in time domain, Eq. (18) is accordingly replaced by the convolution of impulse responses in time domain, Eq. (18) is accordingly replaced by the convolution of $\mathbf{\Delta W}$ and $\mathbf{S}$ that is equal to $\mathbf{\Delta H}$. Hence, Eq. (18) can be rewritten as

$$\mathbf{\Delta H} = \mathbf{PS}, \tag{19}$$

where

$$\mathbf{P}=\begin{bmatrix} w_0(2)-w_0(1) & 0 & \cdots & 0 \\ w_1(2)-w_1(1) & w_0(2)-w_0(1) & \cdots & 0 \\ \vdots & \vdots & \ddots & \vdots \\ w_{L-1}(2)-w_{L-1}(1) & w_{L-2}(2)-w_{L-2}(1) & \cdots & w_0(2)-w_0(1) \end{bmatrix} \tag{20}$$

and it should be noted that N and M must be equal to or greater than L. If $w_0(2)-w_0(1)\neq 0$, that is, $\mathbf{P}$ is a nonsingular matrix, the unknown impulse response of the secondary path can be obtained from Eq. (19) as

$$\mathbf{S}=\mathbf{P}^{-1}\Delta\mathbf{H}. \tag{21}$$

2.2. Online modeling method of the secondary path

It can be noted that to obtain the impulse response of secondary path $\mathbf{S}$ by Eq. (21), the coefficient vectors $\mathbf{W}(1)$, $\mathbf{W}(2)$, $\mathbf{H}(1)$ and $\mathbf{H}(2)$ must be known. Obviously, these vectors can be obtained using offline technology, because the noise control filter can be set arbitrarily prior to starting the active noise control. Eq. (21) can be thus derived by identifying $\mathbf{H}(1)$ and $\mathbf{H}(2)$ that are related to $\mathbf{W}(1)$ and $\mathbf{W}(2)$ set arbitrarily, respectively. Another way to obtain $\mathbf{W}(1)$, $\mathbf{W}(2)$, $\mathbf{H}(1)$ and $\mathbf{H}(2)$ is proposed in Ref. [16]. However, it requires that the updating of the coefficients of $W(z)$ stop, which is not desirable for online secondary path modeling especially in the case that the primary path and secondary path change fast and suddenly. To avoid this, in this section, an effort to obtain Eqs. (4) and (21) online will be made.

In Fig. 5, when applying the FXLMS algorithm, the updating equation of the noise control filter $W(z)$ is

$$\mathbf{W}(n+1)=\mathbf{W}(n)+\mu_W e(n)\left[\hat{S}(z)\mathbf{X}(n)\right], \tag{22}$$

where $\mathbf{W}(n)=\begin{bmatrix} w_0(n) & w_1(n) & \cdots & w_{M-1}(n)\end{bmatrix}^{\mathrm{T}}$ is the coefficient vector of the adaptive filter at time n, $\mathbf{X}(n)=\begin{bmatrix} x(n) & x(n-1) & \cdots & x(n-M+1)\end{bmatrix}^{\mathrm{T}}$, and μ_W is the step size. Here, an error vector is defined as

$$\mathbf{F}(n)=\mathbf{W}(n)-\mathbf{W}^*. \tag{23}$$

According to Eq. (22), we have

$$\begin{aligned}\mathbf{F}(n+1)&=\mathbf{W}(n+1)-\mathbf{W}^* \\ &=\mathbf{F}(n)+\mu_W e(n)\left[\hat{S}(z)\mathbf{X}(n)\right],\end{aligned} \tag{24}$$

where $\mathbf{W}^*$ is the optimal solution of $\mathbf{W}(n)$. From Eqs. (22) and (24), it can be seen that the coefficient vectors of the control filter are different at different iteration steps due to the estimation error. Especially before convergence of $\mathbf{W}(n)$ or error $e(n)$, the estimation error $\mathbf{F}(n)$ is large, and hence the difference between two different iteration steps for specific intervals is large. To utilize the facts, we use the additional filter $H(z)$ to predict and model the overall path $P(z)-W(z)S(z)$ online. Thus, it is required that the estimations of $W(z)$ and $H(z)$ be carried out in parallel, which is feasible if the step sizes of adaptive filters $W(z)$ and $H(z)$ are selected properly. Here, we define

$$W(n,z)=w_0(n)+w_1(n)z^{-1}+w_2(n)z^{-2}+\cdots+w_{M-1}(n)z^{-(M-1)}, \tag{25}$$

$$H(n,z)=h_0(n)+h_1(n)z^{-1}+h_2(n)z^{-2}+\cdots+h_{N-1}(n)z^{-(N-1)} \tag{26}$$

to express the transfer functions $W(z)$ and $H(z)$ at time n. In ideal case, $H(n,z)$ is expected to converge to $P(z)-W(n,z)S(z)$, that is

$$H(n,z)=P(z)-W(n,z)S(z). \tag{27}$$

According to Eq. (27), for any two different iteration times, such as the time $n-k$ and time $n-m$ (where $k = 0, 1, 2, \ldots$; $m = 0, 1, 2, \ldots$; and $k \neq m$), the simultaneous equations can be obtained as

$$H(n-k,z) = P(z) - W(n-k,z)S(z) \tag{28}$$

and

$$H(n-m,z) = P(z) - W(n-m,z)S(z). \tag{29}$$

On the assumption that $k<m$ and the characteristics of the secondary path and primary path would not change between the time $n-m$ and time $n-k$, eliminating $P(z)$ from Eqs. (28) and (29) yields

$$S(z) = \frac{H(n-k,z) - H(n-m,z)}{W(n-m,z) - W(n-k,z)} \tag{30}$$

if $W(n-m, z) - W(n-k, z) \neq 0$. Similar to the derivation of Eq. (21), the impulse response of the secondary path can be online derived as

$$\mathbf{S} = \mathbf{P}^{-1}(n)\Delta\mathbf{H}(n), \tag{31}$$

where

$$\begin{aligned}\Delta\mathbf{H}(n) &= \mathbf{H}(n-k) - \mathbf{H}(n-m)\\ &= \big[\, h_0(n-k) - h_0(n-m) \quad h_1(n-k) - h_1(n-m)\\ &\quad \cdots \quad h_{N-1}(n-k) - h_{N-1}(n-m) \,\big]^{\mathrm{T}},\end{aligned} \tag{32}$$

$$\mathbf{P}(n) = \begin{bmatrix} w_0(n-m) - w_0(n-k) & 0 & \cdots & 0 \\ w_1(n-m) - w_1(n-k) & w_0(n-m) - w_0(n-k) & \cdots & 0 \\ \vdots & \vdots & \ddots & \vdots \\ w_{L-1}(n-m) - w_{L-1}(n-k) & w_{L-2}(n-m) - w_{L-2}(n-k) & \cdots & w_0(n-m) - w_0(n-k) \end{bmatrix} \tag{33}$$

and $w_0(n-m) - w_0(n-k) \neq 0$.

2.3. Implementation considerations of the algorithm

Eq. (30) has been obtained by online method, and the secondary path can be estimated by Eq. (31), theoretically. However, some problems need to be considered for specific implementation.

In practical ANC systems using a DSP board as the real-time controller, the computational load and memory requirement are the main considerations for the choice of control algorithms. Heavy computational burden and large memory requirement can increase the burden of the controller, and are directly related to the increment of hardware cost. A good improved ANC algorithm should be one whose computational load is much less than existing algorithms without deterioration in performance, such as the Delayed-X LMS algorithm [17]. It can be seen from Eq. (33) that $\mathbf{P}(n)$ is an $L \times L$ matrix, and so its matrix inverse $\mathbf{P}^{-1}(n)$ is also an $L \times L$ matrix. Thus, huge memory is needed to obtain $\mathbf{P}(n)$, especially when L is large. The matrix $\mathbf{P}^{-1}(n)$ needs to be computed online with the updation of $\mathbf{W}(n)$ at each adaptation step. In addition, the computation of $\mathbf{P}^{-1}(n)\Delta\mathbf{H}(n)$ in Eq. (31) also needs $L \times L$ multiplication/addition operations. Therefore, modeling the secondary path online by Eq. (31) needs much memory and the computatonal load is heavy.

Eq. (27) is derived on the hypothesis of $H(n, z)$ modeling $P(z) - W(n, z)S(z)$ ideally. In fact, however, $P(z) - W(n, z)S(z)$ is estimated by $H(n, z)$ approximately. Therefore, some estimation errors are included in $\mathbf{H}(n)$, and transferred to $\Delta\mathbf{H}(n)$. The errors will pile up with every solution from s_0 to s_L, and may cause the updation diverge eventually.

In addition, $w_0(n-m) - w_0(n-k)$ may be zero because it is a random variable, during the control process. Hence, the condition $w_0(n-m) - w_0(n-k) \neq 0$ cannot be satisfied, and the impulse response of the secondary path cannot be solved by Eq. (31).

2.4. System identification technique

In this section, a new system identification technique is adopted to solve the problems mentioned above. Eq. (30) shows that $H(n-k, z) - H(n-m, z)$ is equal to the product of $W(n-m, z) - W(n-k, z)$ and $S(z)$. If an adaptive filter $\hat{S}(z)$ is introduced and the coefficients of the adaptive filter are updated by LMS algorithm so that the output of $H(n-k, z) - H(n-m, z)$ is equal to the output of the product of $\hat{S}(z)$ and $W(n-m, z) - W(n-k, z)$, then adaptive filter $\hat{S}(z)$ is expected to converge on $S(z)$ with some errors. Therefore, the system identification technique can be illustrated in Fig. 6, in which the identification operation of the secondary path is parallel to operation of the active noise control process. An FIR filter is selected as the adaptive filter here. Since all adaptive filter coefficients are simultaneously updated, the estimation error contained in $H(n-k, z) - H(n-m, z)$ is widely and uniformly distributed over the coefficients of the adaptive filter, and so the errors don't diverge. The estimation error contained in $H(n-k, z) - H(n-m, z)$, which is expressed as $R(n, z)$, is transferred to $\hat{S}(z)$. Accordingly, indeed, $\hat{S}(z)$ will converge on

$$\hat{S}(z) = S(z) + S'(n, z) + R(n, z), \tag{34}$$

where $S'(n, z)$ is the identification error of $\hat{S}(z)$ itself. So the estimation precision of $S(z)$ is limited to an extent in the proposed method because of the inherent estimation error $R(n, z)$ in $H(n-k, z) - H(n-m, z)$.

In frequency domain the reference signal $x(n)$ and Eq. (30) can be expressed as $X(e^{jw})$ and

$$S(e^{jw}) = \frac{H(n-k, e^{jw}) - H(n-m, e^{jw})}{W(n-m, e^{jw}) - W(n-k, e^{jw})}, \tag{35}$$

respectively. From the derivation of Eq. (30), one can know that Eq. (35) comes into being only in the frequency domain of the reference signal $X(e^{jw})$. In other words, $H(n, z)$ only can model $P(z) - W(n, z)S(z)$ in

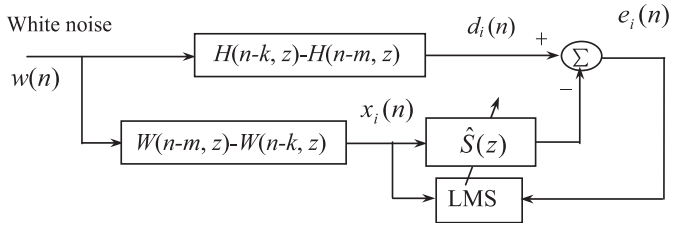

Fig. 6. System identification strategy to solve Eq. (30).

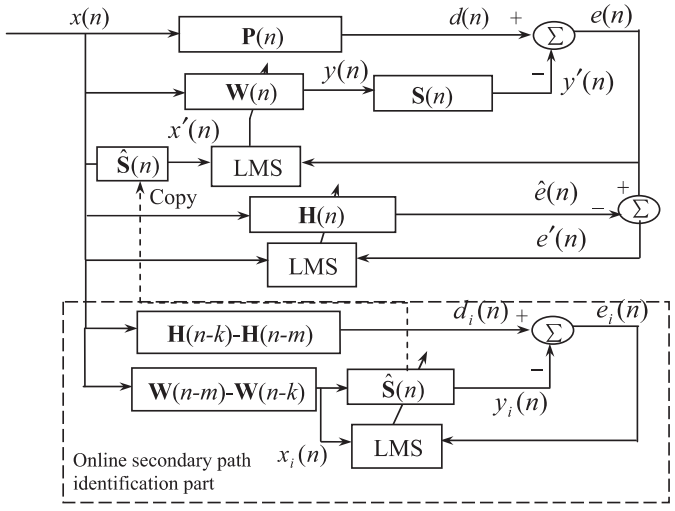

Fig. 7. Block diagram of ANC system with proposed online secondary path modeling method.

the frequency range of $X(e^{jw})$. Even if the white noise is used as the input of the identification system, as shown in Fig. 6, the secondary path model for the entire frequency domain cannot be obtained. Furthermore, it is known to us that in order to attenuate the primary noise correlated with the reference signal, the secondary path only needs to be estimated in the frequency range of the reference signal $X(e^{jw})$. More importantly, the system identification part is separated from the ANC part. Therefore, the reference signal may be used as the input of the identification system, which simplifies the ANC system. The proposed algorithm can be further illustrated in Fig. 7.

In Fig. 7, the proposed algorithm requires three adaptive filters, i.e., the noise control filter $\mathbf{W}(n)$, additional filter $\mathbf{H}(n)$, and the secondary path modeling filter $\hat{\mathbf{S}}(n)$ to run online, and to be updated simultaneously at each adaptation step. The updating equation of $\mathbf{W}(n)$ is shown in Eq. (22), the updating equations of $\mathbf{H}(n)$ and $\hat{\mathbf{S}}(n)$ are

$$\mathbf{H}(n+1) = \mathbf{H}(n) + \mu_H \mathbf{X}(n) e'(n), \tag{36}$$

where μ_H is the step size of $\mathbf{H}(n)$,

$$e'(n) = e(n) - \hat{e}(n) = d(n) - y'(n) - \mathbf{X}^{\mathrm{T}}(n)\mathbf{H}(n), \tag{37}$$

$$\hat{\mathbf{S}}(n+1) = \hat{\mathbf{S}}(n) + \mu_S \mathbf{X}_i(n) e_i(n), \tag{38}$$

where μ_S is the step size of $\hat{\mathbf{S}}(n)$, $\mathbf{X}_i(n) = [\,x_i(n) \quad x_i(n-1) \quad \cdots \quad x_i(n-L+1)\,]^{\mathrm{T}}$,

$$e_i(n) = d_i(n) - y_i(n) = d_i(n) - \mathbf{X}_i^{\mathrm{T}}(n)\hat{\mathbf{S}}(n), \tag{39}$$

$$d_i(n) = \mathbf{X}^{\mathrm{T}}(n)\Delta\mathbf{H}(n), \tag{40}$$

$$x_i(n) = \mathbf{X}^{\mathrm{T}}(n)\Delta\mathbf{W}(n), \tag{41}$$

where $\Delta\mathbf{W}(n) = \mathbf{W}(n-m) - \mathbf{W}(n-k)$, $\Delta\mathbf{H}(n) = \mathbf{H}(n-k) - \mathbf{H}(n-m)$. The operation procedure of the proposed algorithm is summarized as follows:

(1) At time $n = 0$, the algorithm is initialized first. The initial coefficients vectors of adaptive filters, $\mathbf{W}(n)$ and $\mathbf{H}(n)$, are set to be 0, respectively, $\hat{\mathbf{S}}(n)$ is set to be $\mathbf{S}(0) = [\,a \quad 0 \quad \cdots \quad 0\,]^{\mathrm{T}}$, and $a \neq 0$.
(2) At time n, the coefficient vectors $\mathbf{H}(n-k)$, $\mathbf{H}(n-m)$, $\mathbf{W}(n-k)$ and $\mathbf{W}(n-m)$ (when $n \leqslant k$, $\mathbf{H}(n-k)$, $\mathbf{H}(n-m)$, $\mathbf{W}(n-k)$ and $\mathbf{W}(n-m)$ are all zero vectors; when $k \leqslant n \leqslant m$, $\mathbf{H}(n-m)$ and $\mathbf{W}(n-m)$ are zero vectors) are obtained. Then $\Delta\mathbf{W}(n) = \mathbf{W}(n-m) - \mathbf{W}(n-k)$ and $\Delta\mathbf{H}(n) = \mathbf{H}(n-k) - \mathbf{H}(n-m)$ are computed. $\mathbf{W}(n)$ and $\mathbf{H}(n)$ are updated by Eqs. (22) and (36), respectively.
(3) Compute $d_i(n)$, $y_i(n)$ and $d_i(n)$, update $\hat{\mathbf{S}}(n)$ by Eq. (38).
(4) At time $n+1$, repeat operations (2) and (3).

From Fig. 7 and the operation procedure of the algorithm, it should be noted that it is necessary to set the initial coefficients of $\hat{\mathbf{S}}(n)$ to be a nonzero vector to ensure the algorithm to work. For convenience, $\hat{\mathbf{S}}(0) = [\,a \quad 0 \quad \cdots \quad 0\,]^{\mathrm{T}}$ or $\hat{\mathbf{S}}(0) = [\,0 \quad 0 \quad \cdots \quad a\,]^{\mathrm{T}}$ is usually set. Table 1 presents the computational loads (number of multiplication/addition operations) of the ANC system with the proposed algorithm and other secondary path modeling algorithms. For brevity, in Table 1 and the following sections, the online secondary path

Table 1
A comparison of computational loads of the proposed algorithm and other modeling methods

ANC system with online secondary path modeling algorithm	Multiplication/addition operations		
Constant injection noise method (Zhang's method)	$2M+2N+3L$		
Variable injection noise method (Lan's method)	$2M+2N+3L+1$		
Proposed algorithm	$3M+3N+3L$		
Simultaneous equation method (Fujii's method)	When updating $W(z)$	Updating $H(z)$	Estimating $\hat{S}(z)$
	$2M+L$	$M+2N$	$K(M+N+2L)$

modeling algorithms using injection noise in Refs. [7,11] are called constant injection noise method and variable injection noise method, respectively, according to the characteristics of their injected noise. In this table, M, L, and N are the lengths of the control filter $W(z)$, secondary path modeling filter $\hat{S}(z)$, and the additional filter $H(z)$, respectively. It is necessary to point out that in the simultaneous equation method in Ref. [16], $W(z)$, $H(z)$ and $\hat{S}(z)$ are not updated simultaneously at one adaptation step in parallel, but are estimated in three separate processes. So the computational loads in different processes are different, as shown in Table 1 where K is the number of iterations required to estimate $\hat{S}(z)$. It can be seen that the computational load of the proposed algorithm increases slightly compared to that of the modeling methods with injection noise due to the operations in Eqs. (40) and (41), but much lower than that of the process of estimating $\hat{S}(z)$ with Fujii's method, especially when large K is needed to obtain a perfect estimation of $\hat{S}(z)$. In addition, only $2L+M+N$ multiplication/addition operations are needed for updating $\hat{\mathbf{S}}(n)$ at each adaptation step in the secondary path modeling part with the proposed algorithm, which is much less than that of solving Eq. (31).

3. Effects of parameter selection on the algorithm

Eq. (27) is the premise of the proposed algorithm. According to Eq. (34), the online modeling precision of secondary path depends on the estimation error $R(n,z)$. Because the noise control filter $\mathbf{W}(n)$ is updated by Eq. (22), the overall path $P(z)-W(n,z)S(z)$ is a time-varying system. Especially before convergence of the coefficients of $\mathbf{W}(n)$, the time varying is fast. In order to predict and model $P(z)-W(n,z)S(z)$ fast and well by $\mathbf{H}(n)$, the convergence speed of $\mathbf{H}(n)$ should be faster than that of $\mathbf{W}(n)$. So the step sizes of $\mathbf{W}(n)$ and $\mathbf{H}(n)$ should satisfy the condition

$$\mu_H > \mu_W. \tag{42}$$

In Fig. 7, $\mathbf{W}(n-m)-\mathbf{W}(n-k)$ and $\mathbf{H}(n-k)-\mathbf{H}(n-m)$ are the differences of the coefficient vectors of the adaptive filters $W(z)$ and $H(z)$ between the time $n-k$ and time $n-m$. In the ideal case that $P(z)-W(n,z)S(z)$ is modeled by $H(n,z)$ precisely, the difference of the interval $\Delta=(n-m)-(n-k)$ does not result in the difference of the identification results of the secondary path. However, it has been known that $\mathbf{H}(n-k)-\mathbf{H}(n-m)$ includes errors. The different choices of Δ may result in different values of $\mathbf{H}(n-k)-\mathbf{H}(n-m)$ and different proportions of estimation error $R(n,z)$ to $H(n-k,z)-H(n-m,z)$, and thus result in the difference of the identification results. Therefore, it will be discussed in frequency domain how different choices of Δ affect the identification of secondary path in the following section.

If the optimal solutions of $H(n-k,e^{jw})$ and $H(n-m,e^{jw})$ are expressed as $H^*(n-k,e^{jw})$ and $H^*(n-m,e^{jw})$, and the estimation errors contained in $H(n-k,e^{jw})$ and $H(n-m,e^{jw})$ are expressed as $H^r(n-k,e^{jw})$ and $H^r(n-m,e^{jw})$, respectively, then

$$H(n-k,e^{jw}) = H^*(n-k,e^{jw}) + H^r(n-k,e^{jw}), \tag{43}$$

$$H(n-m,e^{jw}) = H^*(n-m,e^{jw}) + H^r(n-m,e^{jw}) \tag{44}$$

and

$$\begin{aligned} &H(n-k,e^{jw}) - H(n-m,e^{jw}) \\ &\quad = H^*(n-k,e^{jw}) - H^*(n-m,e^{jw}) + H^r(n-k,e^{jw}) - H^r(n-m,e^{jw}). \end{aligned} \tag{45}$$

Thus, the estimation error contained in $H(n-k,e^{jw})-H(n-m,e^{jw})$ can be expressed as $R(n,e^{jw}) = H^r(n-k,e^{jw})-H^r(n-m,e^{jw})$, which is a perturbation term that can be transformed to a perturbation noise in $d_i(n)$. So $H(n-k,z)-H(n-m,z)$ in Fig. 6 can be decomposed as $H^r(n-k,z)-H^r(n-m,z)$ and $H^*(n-k,z)-H^*(n-m,z)$, and $d_i(n)$ can be decomposed as $d_i^r(n)$ and $d_i^*(n)$, as illustrated in Fig. 8 where $d_i^r(n)$ is the perturbation noise produced by estimation error $R(n,e^{jw})$. Although $d_i^r(n)$ is correlated with the input $x(n)$, it is regarded as a disturbance on $d_i^*(n)$. $R(n,e^{jw})$ or $d_i^r(n)$ can disturb the identification process and degrade the identification performance of the secondary path filter. Here, we define the relative error

$$\xi(n,e^{jw}) = \left|\frac{R(n,e^{jw})}{H^*(n-k,e^{jw}) - H^*(n-m,e^{jw})}\right|. \tag{46}$$

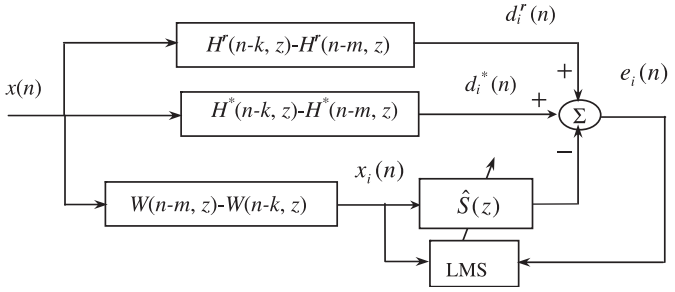

Fig. 8. Block diagram of decomposed system identification strategy to solve Eq. (30) using the reference signal $x(n)$ as the input.

Eq. (46) can be used to explain the effect of different Δ selection on the identification of the secondary path. When Δ is large, the difference $\mathbf{H}(n-k)-\mathbf{H}(n-m)$ is large, and hence $H^*(n-k, e^{jw})-H^*(n-m, e^{jw})$ is large. According to Eq. (46), $\xi(n, e^{jw})$ is small, which indicates the ratio of estimation error $R(n, e^{jw})$ to $H^*(n-k, e^{jw})-H^*(n-m, e^{jw})$ is small, so the influence of error $R(n, e^{jw})$ on the identification of the secondary path is little. From Fig. 8, it can also be known that as the differences $\mathbf{H}(n-k)-\mathbf{H}(n-m)$ and $\mathbf{W}(n-m)-\mathbf{W}(n-k)$ are larger, the term $d_i(n)$ and the excitation signal $x_i(n)$ are larger, and the term $d_i^*(n)$ is also larger. Therefore, the influence of $d_i^r(n)$ on $d_i^*(n)$ becomes less, and the convergence speed and estimation precision of system identification become higher.

Fig. 7 gives the general illustration of the proposed algorithm, in which $\mathbf{H}(n-k)$ is the coefficient vector of $H(z)$ at time $n-k$ that is k steps earlier than the time n. It can be known that $\mathbf{W}(n-m)-\mathbf{W}(n-k)$ and $\mathbf{H}(n-k)-\mathbf{H}(n-m)$ are not nonzero vectors and $\hat{\mathbf{S}}(n)$ is not updated until $\mathbf{H}(n-k)=\mathbf{H}(1)$ and $\mathbf{W}(n-k)=\mathbf{W}(1)$ at time $n=k+1$. The coefficient updating of $\hat{\mathbf{S}}(n)$ is thus delayed k steps. Therefore, k is best chosen as zero so as not to delay the response of the system identification part.

Assuming that $H(n, z)$ is equal to $P(z)-W(n, z)S(z)$ for any time n, one can understand that the vectors $\mathbf{H}(n-k)$ and $\mathbf{W}(n-k)$, k steps earlier than the time n, and the vectors $\mathbf{H}(n-m)$ and $\mathbf{W}(n-m)$, m steps earlier than the time n, are needed in order to obtain the entire Eq. (30) and update $\hat{\mathbf{S}}(n)$, if no a sudden change of the secondary path occurs between the interval. However, if the secondary path has a sudden change at the time $n=n-l$ $(k<l<m)$ during the adaptation process between the time $n-m$ and time $n-k$, $\hat{\mathbf{S}}(n)$ will experience wrong adaptations of $m-l$ steps. In fact, $\hat{\mathbf{S}}(n)$ may experience more wrong adaptations than that because it needs a convergence process for $H(n, z)$to estimate $P(z)-W(n, z)S(z)$. From the above analysis, it can be known that the larger Δ, i.e., the larger the time spans of Eq. (30), the slower the response of the online identification system to sudden change of the secondary path is.

Here, it is necessary to point out that the initial wrong adaptations of $\hat{\mathbf{S}}(n)$ are not harmful to the online modeling of the secondary path for the proposed algorithm. This is because the wrong adaptations of $\mathbf{W}(n)$ caused by the wrong adaptations of $\hat{\mathbf{S}}(n)$ result in the enlargement of $\mathbf{F}(n)$, followed by the magnification of the differences $\mathbf{W}(n-m)-\mathbf{W}(n-k)$ and $\mathbf{H}(n-k)-\mathbf{H}(n-m)$ which further result in the enlargement of $d_i(n)$ and the excitation signal $x_i(n)$, and hence the updating of $\hat{\mathbf{S}}(n)$ is speeded up.

4. Simulation results and discussions

Many computer simulations have been conducted to verify the effectiveness and evaluate the performance of the proposed algorithm. The simulations will be presented in three sections. In the first section, we demonstrate the effect of different choices of interval Δ on the online secondary path identification. In the second section, we demonstrate the modeling performance of the proposed algorithm. In the third section, we demonstrate the control effect with the online secondary path modeling.

In the simulations, the models of the primary path and secondary path are all chosen as the FIR filter models. The primary acoustic path is

$$P(z)=0.8z^{-9}+0.6z^{-10}-0.2z^{-11}-0.5z^{-12}-0.1z^{-13}+0.4z^{-14}-0.05^{-15}. \quad (47)$$

The secondary acoustic path is

$$S(z) = z^{-5} + 2.5z^{-6} + 1.76z^{-7} + 0.15z^{-8} - 0.4825z^{-9} - 0.18625z^{-10} - 0.005^{-11}. \quad (48)$$

There is a zero $z = 1.5$ outside the unit circle and five samples delay in the secondary path, which is a non-minimum-phase system. It contains the main characteristics of the real secondary path. The sampling frequency used for simulations is set at 2000 Hz. The initial values of the adaptive filters $\mathbf{W}(n)$ and $\mathbf{H}(n)$ are set to zeros. The initial value of $\hat{\mathbf{S}}(n)$ is $\mathbf{S}(0) = [1 \quad 0 \quad \cdots \quad 0]^{\mathrm{T}}$. The normalized versons of FXLMS and LMS algorithms are used. The filtered-X NLMS (FXNLMS) algorithm is used to update $\mathbf{W}(n)$, and NLMS algorithm used to update $\mathbf{H}(n)$ and $\hat{\mathbf{S}}(n)$.

4.1. Effect of interval Δ on online secondary path modeling

The parameters used in the section are selected as follows: the adaptive filter length is $L = M = N = 12$, the primary noise $x(n)$ is assumed to be a sinusoid wave of unitary amplitude with frequency 230 Hz, the step sizes for updating $\mathbf{W}(n)$, $\mathbf{H}(n)$ and $\hat{\mathbf{S}}(n)$ are $\mu_W = 0.005$, $\mu_H = 0.2$, and $\mu_S = 0.01$, respectively, and k is chosen as zero. Fig. 9 shows the estimation errors of the secondary path versus interval Δ. Here, only the simulation results for Δ from 0 to 120 are given, and the estimation errors shown in Fig. 9 are the absolute errors.

It can be seen that the magnitude and phase errors are large and the fluctuating of the errors is also large with different Δ when Δ is small. This indicates that the influence of the error $R(n, e^{jw})$ on the identification of the secondary path is great when Δ is small. As Δ gets larger, the influence becomes less, so both the estimation errors and the fluctuating of the errors become small. When $\Delta = 1$, the phase estimation error reaches 37°, however the FXNLMS algorithm can converge due to the robustness of the algorithm itself, because the error is less than 90° [18].

Fig. 10(a) shows the time history of the residual error $e(n)$ when $\Delta = 15$. Fig. 10(b) shows the time history of the residual error $e(n)$ when $\Delta = 120$. The secondary path has a sudden change during the control process. The first and second nonzero samples of the impulse response of secondary path change from 1 and 2.5 to 2 and 5.5, respectively, at the 2000th iteration. From the results in Fig. 10, it can be found that the residual errors all have good convergence behavior in the two cases, which shows that the influence of the secondary path can be compensated effectively by the proposed algorithm. But the time of starting converging for $\Delta = 120$ is later than that for $\Delta = 15$, which confirms the conclusion that the larger the Δ, the slower the response of the identification system to a sudden change of the secondary path is.

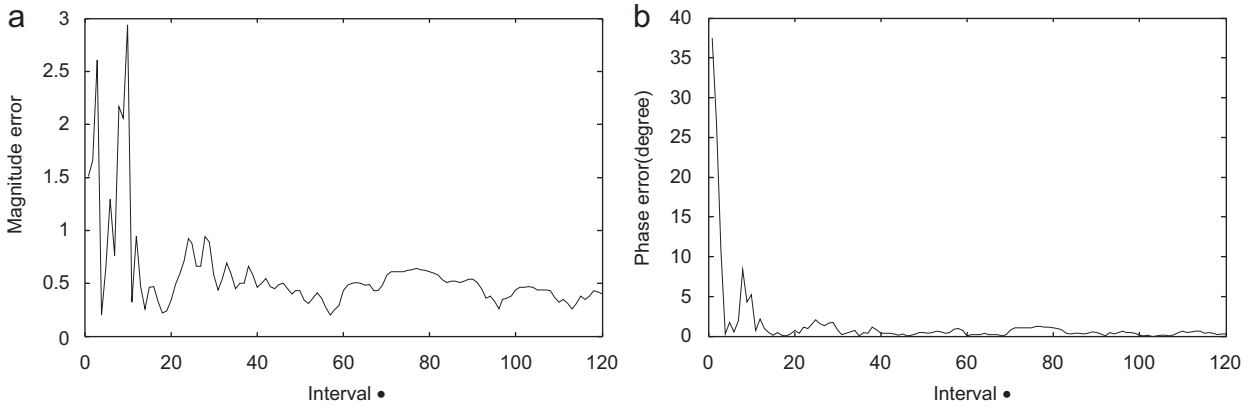

Fig. 9. The estimation error of the secondary path for different interval Δ at frequency 230 Hz with the proposed algorithm: (a) magnitude error; (b) phase error.

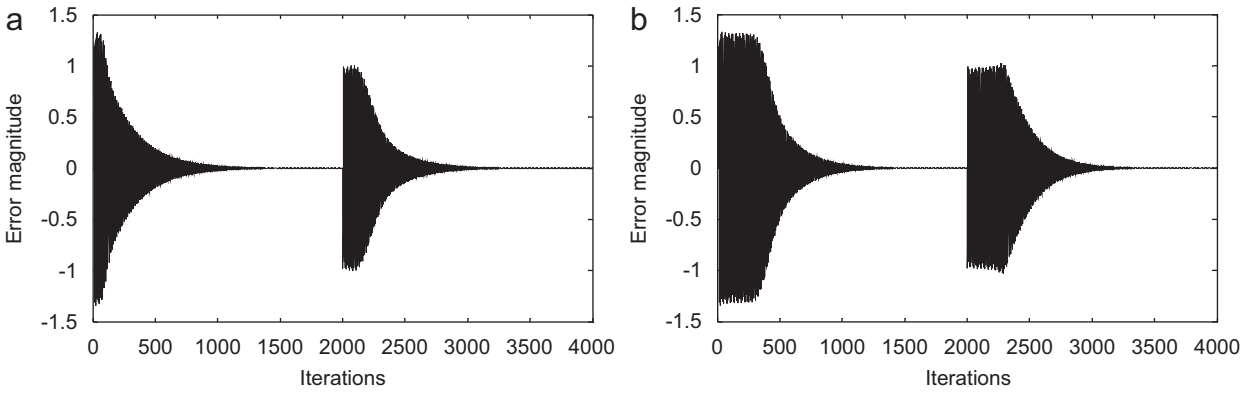

Fig. 10. Time history of the residual error $e(n)$ for different interval Δ: (a) $\Delta = 15$; (b) $\Delta = 120$. The secondary path has a sudden change at the 2000th iteration.

4.2. Modeling performance of the proposed algorithm

In this section, the reference signal $x(n)$ is assumed to be a zero-mean white noise with power of 0.1. For convenience, the adaptive filter lengths are selected as $L = M = N = 40$. Other parameters are the same as those in the simulations of the last section. To evaluate the modeling performance of the proposed algorithm, the secondary path is first modeled with a 40-tap adaptive filter offline, and then online estimated impulse responses of the secondary path are compared with the offline estimated model.

Fig. 11 shows the comparison of online and offline estimated impulse responses of the secondary path. Fig. 12 shows the comparison of frequency responses of online and offline secondary path estimations. From the comparison results, it can be seen that the proposed algorithm can online model the secondary path well in the frequency range concerned.

To demonstrate the convergence behavior of the estimation error, the relative estimation error of the secondary path is defined as $\Delta S(n) = \|\hat{\mathbf{S}}(n) - \mathbf{S}(n)\|^2/\|\mathbf{S}(n)\|^2$. Fig. 13 shows the convergence behavior of the estimation error of the secondary path for different interval Δ. It can be noted that the larger the interval Δ, the better the convergence behavior of the estimation error is. The estimation error curve of $\Delta = 150$ is very similar to that of $\Delta = 120$; however, the difference between the estimation error curve of $\Delta = 60$ and that of $\Delta = 30$ is large. These results again demonstrate that as the interval Δ gets larger, the influence of the error $R(n, e^{jw})$ on the modeling of the secondary path becomes less, so does the influence of the difference of interval Δ on the modeling. The overshoot at the initial updating stage is caused by the wrong adaptations of $\hat{\mathbf{S}}(n)$, as analyzed in Section 3 above.

Modeling performance of the proposed algorithm is compared by simulations with that of the online modeling algorithms with injection noise listed in Table 1. It should be mentioned that the Fujii's method proposed in Ref. [16] isn't included here, since in Fujii's method, $W(z)$, $H(z)$ and $\hat{S}(z)$ are not updated simultaneously at one adaptation step in parallel, but are estimated in three separate processes, and it is required that the operations of updating $W(z)$ stop for many iterations to estimate the additional filter $H(z)$. Therefore, the updating processes and convergence behaviors of three filters are not continuous, so it is not appropriate to compare the method with the proposed and the injection noise methods. In simulations, for convenience, the lengths of all filters in the algorithms considered are selected as 40 taps. The interval Δ is chosen as 120. The primary noise powers for three algorithms are the same. The initial power of the injected noise is chosen to be the proper ratio to the primary noise for the injection noise methods. Step sizes are 0.005 for the control filter and 0.2 for the additional filter in the three algorithms. Step size for updating the secondary path modeling filter is 0.01 for the proposed algorithm and 0.0254 for the injection noise methods. In total, 0.0254 is the optimal step size to ensure the convergence of the secondary path modeling. Using a higher step size cannot accelerate the convergence speed; on the contrary, it can cause a divergence.

First of all, to show the effect of active noise control operation and the primary noise on the modeling process with injection noise method, the offline modeling of secondary path is carried out. The power of the

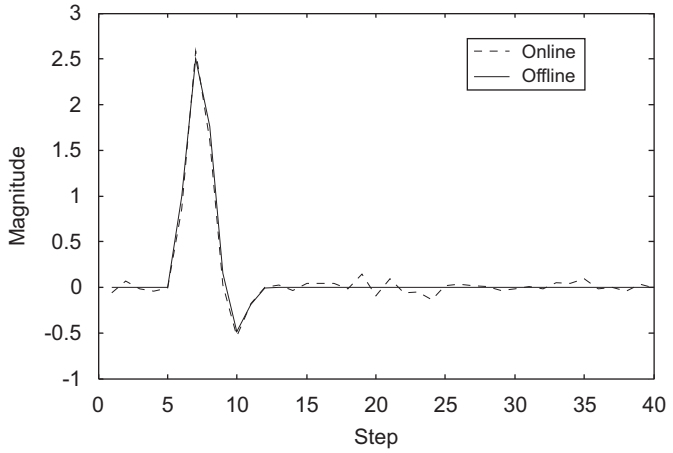

Fig. 11. Comparison of the online modeled impulse response and offline estimated model of the secondary path.

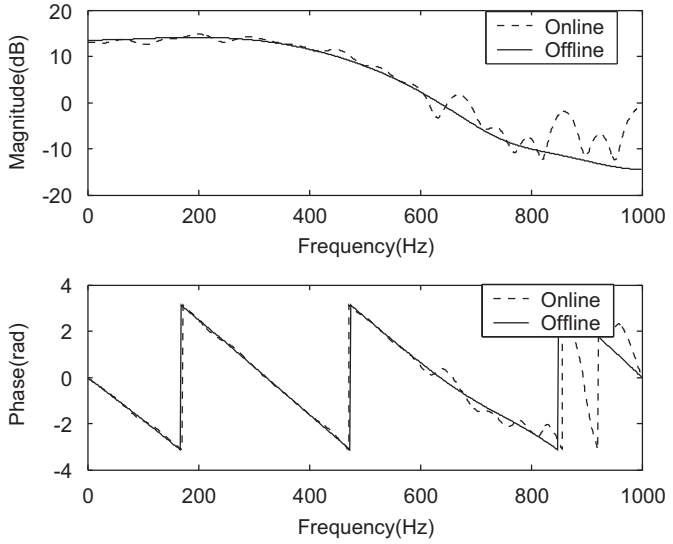

Fig. 12. Comparison of frequency responses of online secondary path estimation and offline estimated model.

white noise and the step size for offline method are the same as those for the online modeling method with injection noise. To demonstrate the robustness of the proposed method and the ability of tracking sudden change of secondary path, two cases where the secondary path changes suddenly are considered. For the first case, the secondary path will experience a sudden change of the amplitude of the impulse response samples at the 10,000th iteration, i.e., the first and second nonzero samples of the impulse response change from 1 and 2.5 to 2 and 5.5, respectively. The second case involves the change of the order of secondary path at the 10,000th iteration, i.e., the secondary acoustic path will be changed to

$$S_m(z) = z^{-6} + 5.5z^{-7} + 1.76z^{-8} + 0.15z^{-9} - 0.4825z^{-10} - 0.18625z^{-11} + 1.2875z^{-12} + 0.15z^{-13} + 0.001875z^{-14},$$

where the length of the FIR filter model of secondary path is increased from 12 to 15, the samples delay is increased from 5 to 6, and the amplitudes of the coefficients of filter model are also changed. The second case corresponds to the change of the position of microphone or speaker in practice.

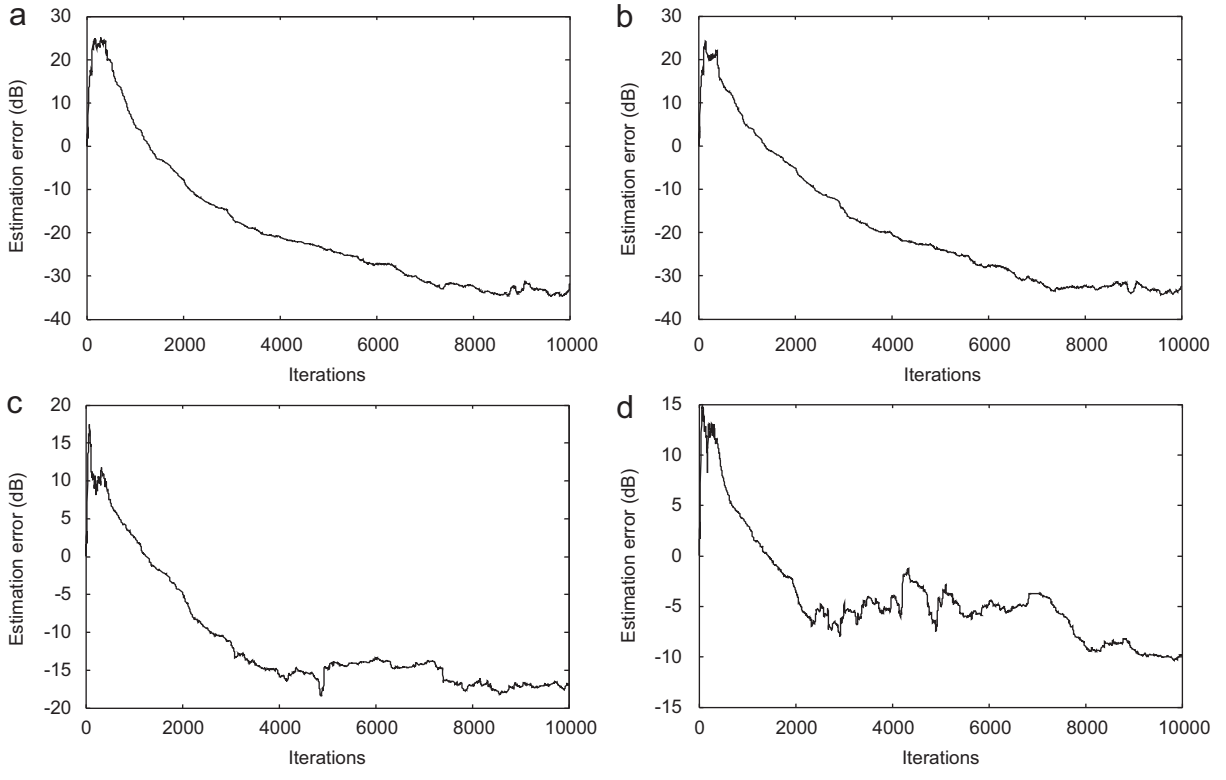

Fig. 13. Convergence behavior of the estimation error of the secondary path for different interval Δ: (a) $\Delta = 150$; (b) $\Delta = 120$; (c) $\Delta = 60$; (d) $\Delta = 30$.

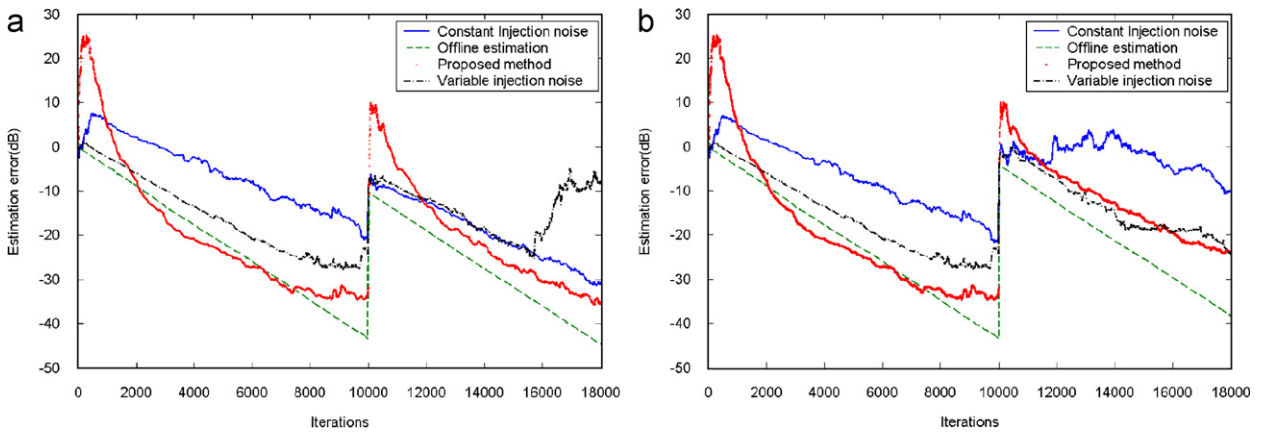

Fig. 14. Comparison of convergence behaviors of the estimation error of secondary path with different modeling methods with a sudden change in the secondary path at the 10,000th iteration: (a) with a change of the amplitude of the impulse response of secondary path; (b) with a change of the order of secondary path.

Fig. 14 presents the comparison of convergence behaviors of the estimation error of secondary path for different modeling methods over this period of 18,000 iterations. Fig. 14(a) and (b) corresponds to the first and second cases of the changes of secondary path, respectively. It is clear that the convergence behavior of the proposed algorithm is different from the other modeling methods. The estimation error with the proposed algorithm shows larger overshoots at initial updating stage and after sudden change than that of the modeling methods with injection noise. However, the proposed method can converge faster and more stably after the

overshoots. This demonstrates that the proposed algorithm can track the sudden change of secondary path fast. The overshoot with the proposed method is again due to the wrong adaptations of $\hat{\mathbf{S}}(n)$, which is helpful to speed up the convergence of the algorithm, as mentioned earlier. For the methods with the injection of auxiliary noise, the operation of ANC controller and the primary noise have a large effect on the secondary path modeling process, as shown in Fig. 14, especially for the constant injection noise method in the case of Fig. 14(b). In addition, it can be seen that the variable injection noise method performs better and is closer to the offline modeling than the constant injection noise method at the initial stage and before convergence; however it may tend to be unstable with the increase of iterations, as the first case in Fig. 14(a). This is because before convergence, the injected noise is large, so the method converges fast and well, however the injected noise is reduced greatly after the system converges. The estimation precision of the proposed algorithm is limited to about 35 dB because of the inherent estimation error $R(n, z)$. The injection noise method has higher estimation precision since it is a signal-independent modeling method [7]. But the precision of 35 dB is enough to ensure the convergence of the FXNLMS algorithm because of its robustness.

Fig. 15 shows the convergence behavior of the coefficients of secondary path modeling filter $\hat{\mathbf{S}}(n)$ using different modeling methods with a sudden change of the amplitude of the impulse response of secondary path. Fig. 16 shows the convergence behavior of the coefficients with the sudden change of the order of secondary path. Fig. 15(a)–(c) corresponds to the first nonzero coefficient, the second nonzero coefficient, and the third nonzero coefficient of the modeling filter $\hat{\mathbf{S}}(n)$, respectively. Fig. 16(a)–(c) corresponds to the second nonzero coefficient, the third nonzero coefficient, and the fourth nonzero coefficient of $\hat{\mathbf{S}}(n)$, respectively. It can be seen that in the two cases, the proposed algorithm can track and converge faster and more stably than the other two online modeling methods after some large fluctuations at the initial stage or after the sudden changes. The fluctuations correspond to the overshoots of the estimation error in Fig. 14, and the reason for that has been

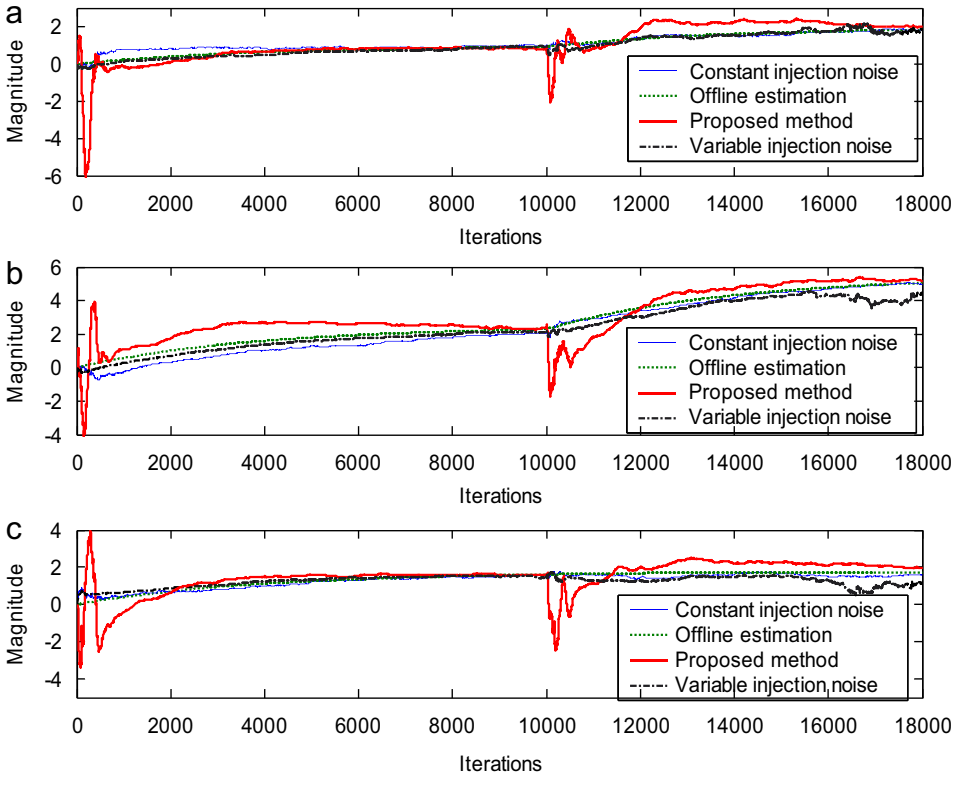

Fig. 15. Convergence behavior of the coefficients of the secondary path modeling filter $\hat{\mathbf{S}}(n)$ using different secondary path modeling methods: (a) the first nonzero coefficient; (b) the second nonzero coefficient; (c) the third nonzero coefficient, with a sudden change of the amplitude of the impulse response of secondary path at the 10,000th iteration.

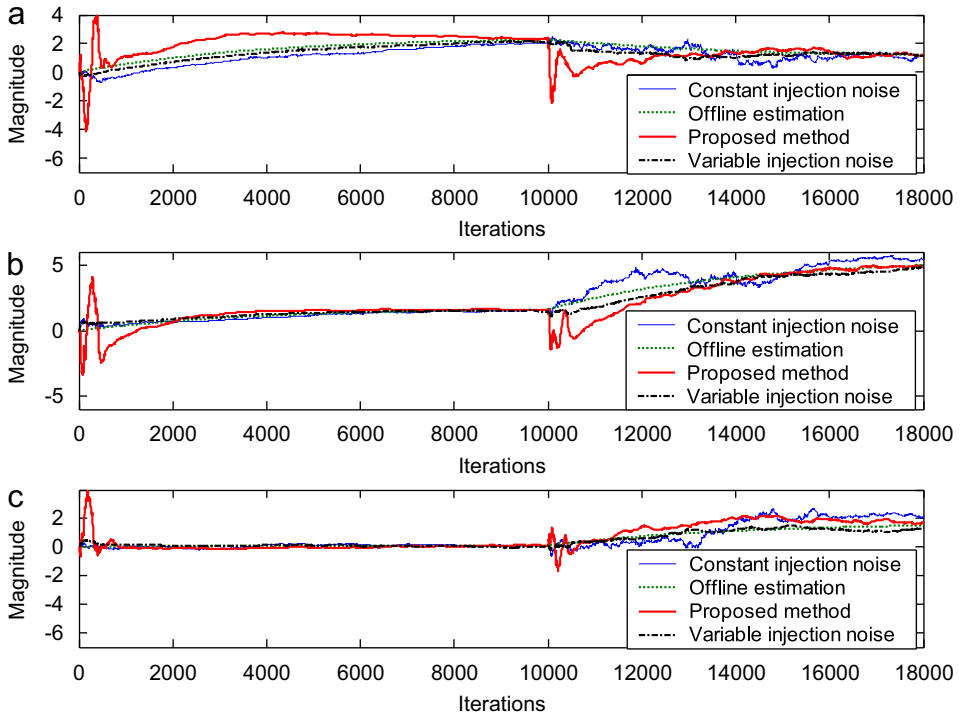

Fig. 16. Convergence behavior of the coefficients of the secondary path modeling filter $\hat{\mathbf{S}}(n)$ using different secondary path modeling methods: (a) the second nonzero coefficient; (b) the third nonzero coefficient; (c) the fourth nonzero coefficient, with a sudden change of the order of secondary path at the 10,000th iteration.

explained above. At the same time, it is seen that the operation of ANC controller and the primary noise have a large effect on the convergence of the coefficients of modeling filter for the constant injection noise method in the second case in Fig. 16. In addition, it can be found that the convergence behaviors of the coefficients for the variable injection noise method perform better and are closer to the offline modeling than that with the constant injection noise method at the initial stage and before convergence; however, they tends to be unstable with the increase of iterations in the first case in Fig. 15. This reason has been explained above. The presented results verify the conclusions drawn from Fig. 14.

4.3. Noise attenuation performance of the ANC system with online secondary path modeling

Noise attenuation effect for a harmonic noise with the proposed algorithm has been shown in Fig. 10. In the section, noise attenuation performance of the broadband ANC system with the proposed algorithm is evaluated by simulations. The parameters and the primary noise power are the same as those in the last section. Fig. 17 shows the time history of the residual error $e(n)$ for two different Δ. It can be seen that the convergence speed of the residual error for $\Delta = 30$ is slower than that for $\Delta = 120$ due to the larger fluctuating during the estimation process of secondary path, as shown in Fig. 13(d).

Fig. 18 shows the time history of the residual error $e(n)$ for $\Delta = 120$ with three different online modeling algorithms over this period of 36,000 iterations, during which the secondary path experiences a sudden change of the amplitude at the 18,000th iteration. It is very clear that the convergence speed of the residual error with proposed algorithm is much faster than that with injection noise methods, and a much lower residual error can be obtained.

The spectrums of the residual error $e(n)$ at the 18,000th iteration for $\Delta = 30$ and 120 are presented in Fig. 19 with the 50 number of spectral averages. The results exhibit good noise attenuation in the frequency range of interest. This shows that the influence of the secondary path on FXNLMS algorithm is compensated

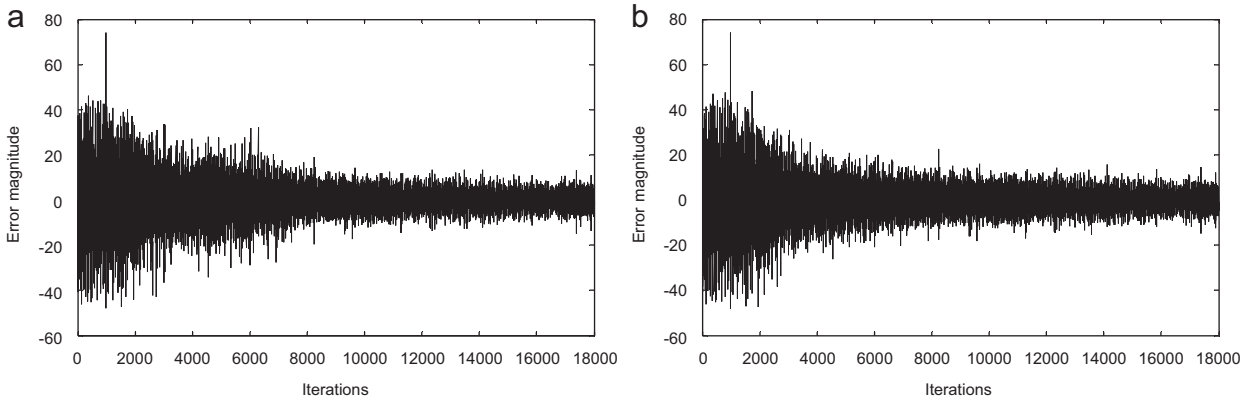

Fig. 17. Time history of the residual error $e(n)$ for different interval Δ: (a) $\Delta = 30$; (b) $\Delta = 120$.

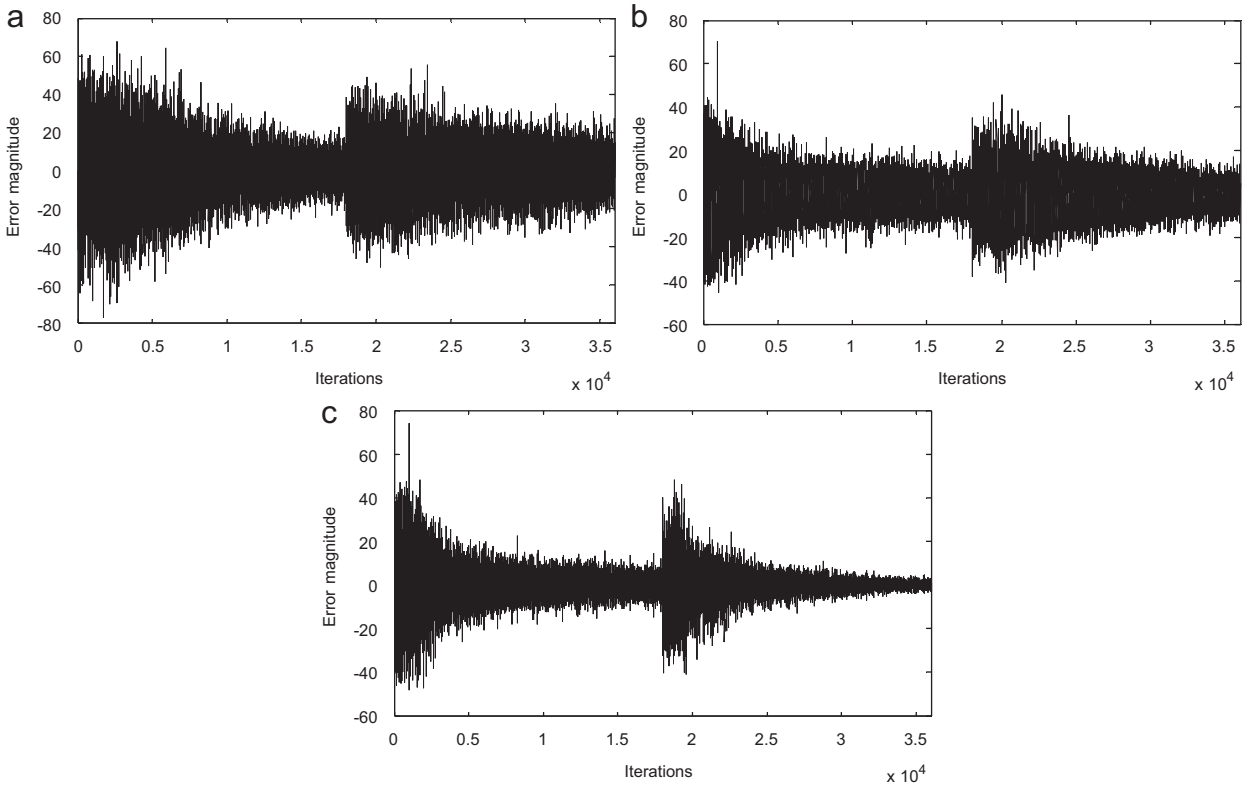

Fig. 18. Time history of the residual error $e(n)$ with different online secondary path modeling algorithms: (a) constant injection noise method; (b) variable injection noise method; (c) proposed method. The secondary path has a sudden change at the 18,000th iteration.

effectively by the proposed algorithm. In addition, combining Figs. 13, 16 and 18, it should be noted that although the estimation error of the secondary path is larger for $\Delta = 30$, the noise attenuation isn't much worse than that for $\Delta = 120$ when the residual errors converge at the stable level after18,000 iterations. This is attributed to the robustness of FXNLMS algorithm. Fig. 20 shows a comparison of the spectrums of the residual error $e(n)$ with two injection noise algorithms. It can be seen that the variable injection noise method can obtain lower residual error than the constant injection noise one. However, comparing Figs. 19 and 20, it is clear that ANC system with proposed algorithm exhibits the best broadband noise attenuation performance.

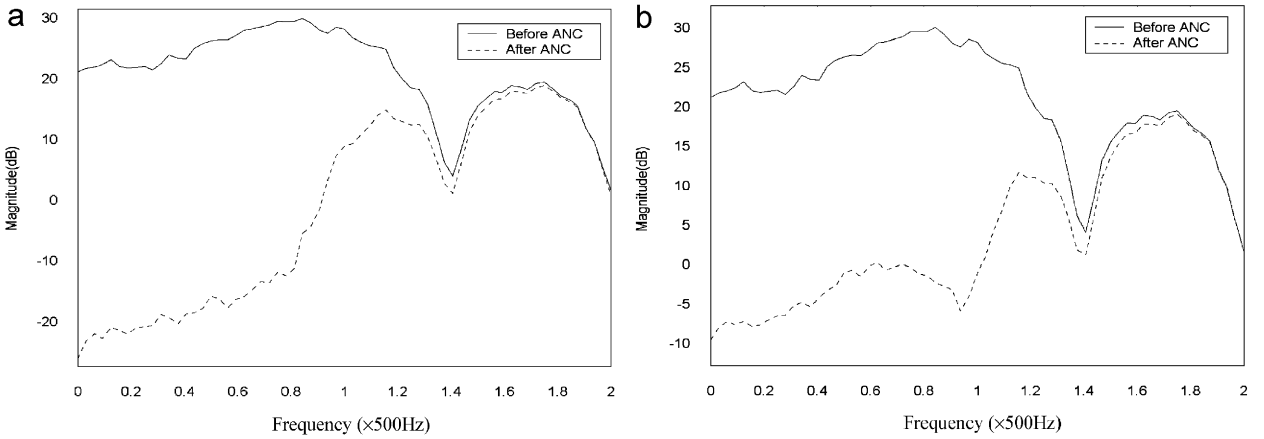

Fig. 19. Spectrum of the residual error $e(n)$ at the 18,000th iteration: (a) $\Delta = 120$; (b) $\Delta = 30$; with the proposed online secondary path modeling method.

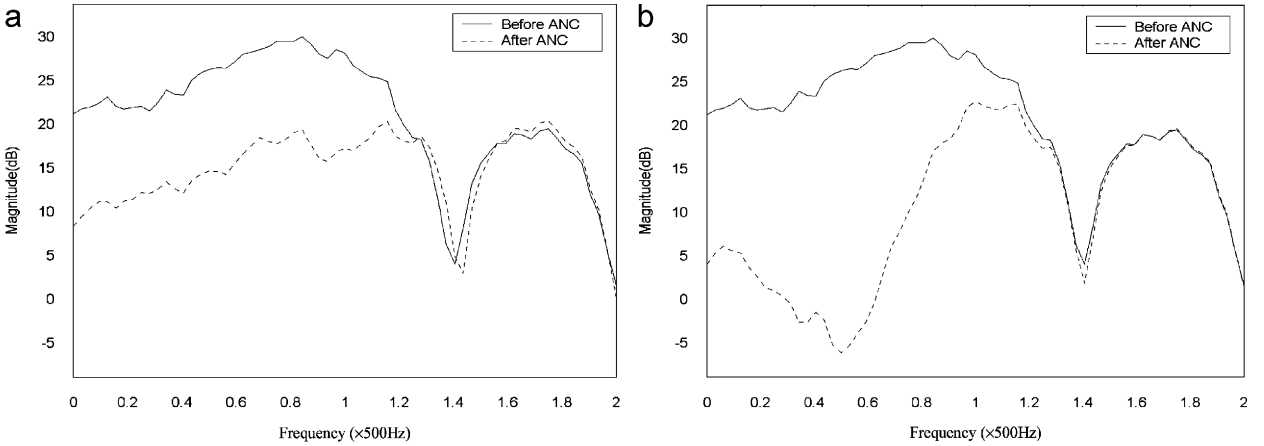

Fig. 20. Spectrum of the residual error $e(n)$ at the 18,000th iteration with different online secondary path modeling methods using injection noise: (a) with the constant injection noise method; (b) with the variable injection noise method.

The results demonstrate that the proposed online modeling algorithm has the distinct advantage of reducing the residual noise greatly.

5. Conclusions

The existing conventional online secondary path modeling algorithms have the characteristics that the operation of the ANC controller and the modeling of the secondary path are mutually interfered. The unwanted disturbances can badly affect the performance of the system, and the disturbances cannot be eliminated radically. A new online secondary path modeling algorithm has been proposed. The method does not need feeding extra noise to the secondary source and also is different from the overall modeling method using the control output. It utilizes the fact that some estimation errors are included in the control filter during the process of updating. In the method, the modeling of the secondary path is relatively independent of the active noise control system, and the reference signal is used as the input for the system identification. Thus, the unwanted disturbances between the operation of the ANC and the identification of the secondary path are eliminated completely, and the complexity of ANC system is greatly reduced. Some implementation considerations and the effect of parameter selection on the online secondary path modeling have been

discussed. Finally, computer simulations demonstrate that the proposed algorithm is effective. It can compensate the influence of the secondary path, and track the sudden change of secondary path. More importantly, it has the distinct advantage of reducing the residual noise greatly. However, since the method is based on the utilization of the estimation errors included in the control filter and the reference signal is used as the input for the system identification, this algorithm has the disadvantages of slow and unstable adaptation and possibility to lose tracking of $W(z)$ and $S(z)$, compared with the signal-independent modeling approach with injection of an auxiliary noise.

References

[1] S.M. Kuo, D.R. Morgan, *Active Noise Control Systems: Algorithms and DSP Implementations*, Wiley, Inc., New York (Copyright ©1996).
[2] C.C. Boucher, S.J. Elliott, The effects of modeling errors on the performance and stability of active noise control system, *Proceedings of the Recent Advances in Active Control of Sound and Vibration*, 1991, pp. 290–301.
[3] S.D. Snyder, C.H. Hansen, The effects of transfer function estimation errors on the filtered-X LMS algorithm, *IEEE Transactions on Signal Processing* 42 (4) (1999) 950–953.
[4] L.J. Eriksson, M.A. Allie, Use of random noise for online transducer estimate in an adaptive attenuation system, *Journal of the Acoustical Society of America* 85 (1989) 797–802.
[5] C. Bao, P. Sas, H.V. Brussel, Adaptive active control of noise in 3-D reverberant enclosures, *Journal of Sound and Vibration* 161 (1993) 501–514.
[6] S.M. Kuo, D. Vijayan, A secondary path estimate techniques for active noise control systems, *IEEE Transactions on Speech and Audio Processing* 5 (1997) 374–377.
[7] M. Zhang, H. Lan, W. Ser, Cross-updated active noise control system with online secondary path modeling, *IEEE Transactions on Speech and Audio Processing* 9 (5) (2001) 598–602.
[8] C. Bao, P. Sas, H.V. Brussel, Comparison of two on-line identification algorithms for active noise control, *Proceedings of the Recent Advances in Active Control of Sound and Vibration*, 1993, pp. 38–51.
[9] S.M. Kuo, J. Luan, Multiple-channel error path modeling with the interchannel decoupling algorithm, *Proceedings of the Recent Advances in Active Control of Sound and Vibration* (1993) 767–777.
[10] N. Saito, T. Sone, T. Ise, M. Akiho, Optimal on-line modeling of primary and secondary paths in active noise control systems, *Journal of the Acoustical Society of Japan* 17 (6) (1996) 275–282.
[11] H. Lan, M. Zhang, W. Ser, An active noise control system using online secondary path modeling with reduced auxiliary noise, *IEEE Signal Processing Letters* 9 (1) (2002) 16–18.
[12] X.J. Qiu, C.H. Hansen, A modified filtered-X LMS algorithm for active control of periodic noise with on-line cancellation path modeling, *Journal of Low Frequency Noise, Vibration and Active Control* 19 (2000) 35–46.
[13] T.J. Yang, Z.Q. Gu, Active control of structural vibration with on-line secondary path modeling, *Progress in Natural Science* 14 (2004) 511–518.
[14] Q.Z. Zhang, W.S. Gan, A model predictive algorithm for active noise control with online secondary path modeling, *Journal of Sound and Vibration* 270 (2004) 1056–1066.
[15] K. Fujii, M. Muneyasu, T. Taiga, Active noise control by simultaneous equation method without estimation of error path filter coefficients, *IEICE Transactions on Fundamentals* A-J82 (1999) 299–305.
[16] K. Fujii, J. Ohga, Method to update the coefficients of the secondary path filter under active noise control, *Signal Processing* 81 (2001) 381–387.
[17] H.S. Kim, Y. Park, Delayed-X LMS algorithm: an efficient ANC algorithm utilizing robustness of canceling path model, *Journal of Sound and Vibration* 212 (5) (1998) 875–887.
[18] X. Sun, D.S. Chen, Convergence analysis of filtered-X LMS algorithm with secondary path modeling error, *Acta Acustica* 27 (2) (2002) 97–101.